High reliability low jitter 80 kV pulse generator

M. E. Savage and B. S. Stoltzfus

Sandia National Laboratories, Albuquerque, New Mexico 87185, USA

(Received 23 June 2009; published 27 August 2009)

Switching can be considered to be the essence of pulsed power. Time accurate switch/trigger systems with low inductance are useful in many applications. This article describes a unique switch geometry coupled with a low-inductance capacitive energy store. The system provides a fast-rising high voltage pulse into a low impedance load. It can be challenging to generate high voltage (more than 50 kilovolts) into impedances less than 10 Ω, from a low voltage control signal with a fast rise time and high temporal accuracy. The required power amplification is large, and is usually accomplished with multiple stages. The multiple stages can adversely affect the temporal accuracy and the reliability of the system. In the present application, a highly reliable and low jitter trigger generator was required for the *Z* pulsed-power facility [M. E. Savage, L. F. Bennett, D. E. Bliss, W. T. Clark, R. S. Coats,J. M. Elizondo, K. R. LeChien, H. C. Harjes, J. M. Lehr, J. E. Maenchen, D. H. McDaniel, M. F. Pasik, T. D. Pointon, A. C. Owen, D. B. Seidel, D. L. Smith, B. S. Stoltzfus, K. W. Struve, W. A. Stygar, L. K. Warne, and J. R. Woodworth, *2007 IEEE Pulsed Power Conference, Albuquerque, NM* (IEEE, Piscataway, NJ, 2007), p. 979]. The large investment in each *Z* experiment demands low prefire probability and low jitter *simultaneously*. The system described here is based on a 100 kV DC-charged high-pressure spark gap, triggered with an ultraviolet laser. The system uses a single optical path for simultaneously triggering two parallel switches, allowing lower inductance and electrode erosion with a simple optical system. Performance of the system includes 6 ns output rise time into 5.6 Ω, 550 ps one-sigma jitter measured from the 5 V trigger to the high voltage output, and misfire probability less than 10^{-4}. The design of the system and some key measurements will be shown in the paper. We will discuss the design goals related to high reliability and low jitter. While reliability is usually important, and is coupled with jitter, reliability is seldom given more than a qualitative analysis (if any at all). We will show how reliability of the system was calculated, and results of a jitter-reliability tradeoff study. We will describe the behavior of sulfur hexafluoride as the insulating gas in the mildly nonuniform field geometry at pressures of 300 to 500 kPa. We will show the resistance of the arc channels, and show the performance comparisons with normal two-channel operation, and single channel operation.

DOI: 10.1103/PhysRevSTAB.12.080401 PACS numbers: 51.50.+v, 52.25.Mq, 52.75.Kq

I. INTRODUCTION

Pulsed-power high voltage systems often use successive stages of pulse amplification to increase a signal to levels needed to trigger a subsequent stage, ultimately reaching the desired voltage and power level. This is certainly true for megavolt systems in which the initiating signal is of the order of ten volts from a computer-controlled system. The initial stages of the trigger process are often the most problematic because of the lower electric fields (below the electron emission threshold of order 30 kV/mm with reasonable gaps and electrode sharpness) in low voltage switches. On many large single-shot drivers, reliability and time accuracy of the entire system (and therefore each stage) are critical.

An improved primary trigger generator for the 28 MJ refurbished *Z* facility was needed. *Z* demands superior time accuracy from each part of its trigger system for synchronizing with fast diagnostics on a one-nanosecond time scale. The primary trigger generator is required to be charged to its ultimate voltage for time periods up to several minutes, then accept a five-volt trigger signal and produce a fast-rising high voltage output, with one-nanosecond or less temporal uncertainty. The substantial investment in each experiment on such a large facility makes the misfire rate an important factor, and prefire and no-fire probabilities of 10^{-4} or lower are required. Because of the large physical size of the *Z* facility, the output pulse from the primary trigger generator operates into multiple (nine) high voltage 50 Ω cables with transit time much longer than the pulse duration. The primary trigger generator thus effectively operates into a 5.56 Ω resistive load.

Because of the stringent performance and reliability requirements for this system, there were no suitable commercially available pulse generators. The load impedance necessitates a relatively low system inductance (less than 22 nH total) for output rise times less than ten nanoseconds. The low tolerance to misfires and low acceptable jitter requires a stable switch with a strong triggering mechanism.

The system described here meets the rise time, amplitude, jitter, and reliability requirements for the *Z* primary trigger generator. The system uses a low-inductance

switch, capacitors, and feeds (14 nH total) with reliable operation at 100 kV DC charge, and a strong laser triggering mechanism. The system operates routinely with no conditioning (although the laser requires 15 minutes for temperature stabilization of the nonlinear crystals), and has subnanosecond (1 standard deviation) jitter and less than 10^{-4} prefire probability at the same time. The system delivers more than one gigawatt into the 5.56 Ω resistive load with six-nanosecond 10%–90% rise time. The maintenance interval is of the order of 10 000 shots at full voltage and usually involves cleaning or replacement of the final focusing lens.

Appreciable challenges are involved in building fast rise time, low jitter pulse generators. While commercially available multioutput ~100 kV trigger systems have been built in the past, they did not meet the jitter or rise time requirements of the primary trigger generator for *Z*, and were notoriously unreliable. In some situations, particularly large drivers with considerable stored energy, an extremely reliable primary trigger generator is crucial, to prevent inadvertent system firing, or failure to fire. Furthermore, in large drivers, system faults, and even normal operation, can apply appreciable external voltages and currents to the trigger unit. The primary trigger generator must tolerate forward and reverse voltages at least as high as the charge voltage, and currents and late-time current at levels as high as the normal output, without damage.

This paper describes technologies considered for the system, and the chosen design. We will show the manner in which the performance goals were validated. While system jitter is straightforward to measure, predicting and minimizing the prefire rate is more challenging, and for that reason is described in some detail. We will also show results on the observed resistance of the spark channel in different gases and for single and double channel operation.

II. POSSIBLE CONFIGURATIONS

Because no commercial system would meet our requirements, we considered several technology options to build the pulser system. The basic technology options considered were solid-state switches, high vacuum electron tubes, low pressure discharge devices, electrically triggered high-pressure spark gaps, and laser-triggered high-pressure spark gaps.

A. Solid-state switched systems, high vacuum thermionic devices, and low pressure gas switches

Because solid-state switches such as thyristors and bipolar or field effect transistors can be extremely reliable, systems using those devices have considerable appeal. The drawback is the relatively low voltage and low current rise rates available from single devices. Large thyristors can block a few kilovolts per device and can handle the 18 kA peak current required for driving 100 kilovolts into 5.56 Ω. However, thyristors do not presently have the $\frac{di}{dt}$ capability of 2.4×10^{12} A/s required for fast rise time, due to limited plasma spreading rates in large devices. Photoconductive switches [1] can switch tens of kilovolts at one kiloamp or less with low inductance and low jitter, but higher currents can degrade the devices. In general, the fault-handling capability of solid-state devices is well below that of gaseous discharge devices because damage in solid-state devices is usually destructive to the switching element. In situations where it is impractical to protect the solid-state device from externally applied spurious currents and voltages, their application can be problematic.

Modular systems with multiple series and parallel switch elements for driving 17 kilovolts and 7.5 Ω with 20 ns rise time have been built using arrays of readily available solid-state devices [2]. Those systems are scalable to higher voltage, but the size and cost of a modular system scales with energy—quadratically with output voltage, and inversely with output impedance. An 80 kV 5.6 Ω system would be substantially larger physically than alternatives with gaseous conductors, and the issue of protecting the solid-state elements from externally applied current and voltage would remain a development effort.

Hard-tube pulsers (high vacuum devices, e.g., planar triodes) would be relatively inefficient in a low impedance system because of the space charge effects of the required beam current and the associated voltage drop in the on condition. Conventional hard-tube systems require large cathode heater powers. The future commercial availability of large thermionic vacuum tube devices appears to be questionable.

Low pressure devices that can be triggered with 1 kV (for example, thyratrons) and control tens of kilovolts at impedances of tens of ohms have existed for decades [3]. Thyratrons can have short-term jitter of a few nanoseconds, but often have a larger long-term drift, and require large and stable low voltage currents for the filament and reservoir. Thyratrons require warm-up times, and conditioning shots to reach a stable operating point. Commercial 100 kV thyratrons would have an inductance of 75 nH or more. Because the total inductance of the switch system must be 20 nH or less, such a system would require multiple thyratrons in parallel, additional pulse sharpening, or both [4]. In the single-shot application described here, the major advantage of thyratrons (long life in repetitive service) is not exploited.

B. High-pressure gas switches

In high-pressure gas switches, generally low jitter and low misfire rate (especially the rate of prefires) are competing requirements; one can be improved at the expense of the other but they are not separable [5] with a given trigger mechanism. Notably, triggered switches themselves do not intrinsically possess jitter—it is the combined switch and

trigger system parameters (trigger impedance, rise time, peak voltage, etc.) that determine the closure jitter at a given operating point. In gas-filled spark gaps, the prefire rate and jitter are generally monotonic and continuous functions of pressure over a substantial range.

A single arc channel carrying a few kA for tens of nanoseconds will be less than a millimeter in diameter in high-pressure gas [6]. With the return conductor located 100 to 300 mm in radius, the arc inductance will be 1.4 to 1.6 nH per mm. For the rise time requirements, a single arc channel must be 10 mm length or less, to allow for a total switch, capacitor, and feed inductance below 25 nH. Five to ten mm gaps in moderately high-pressure (up to 4 bar) sulfur hexafluoride can withstand the required 100 kV DC charge voltage [7].

High-pressure gas switches have some properties that affect their use in such a system. A few of those properties are highlighted below.

(i) The self-breakdown voltage of a high-pressure gas switch at a given pressure is not a constant in general, but rather is best described by a distribution function. The prefire probability of a triggered gas switch at a given set of conditions is largely determined by that self-breakdown distribution function [7–10]. The jitter is usually a function of the fraction of the median self-break voltage (the voltage at which the probability of self-break is 50%) for a given trigger magnitude; switches operated closer to the self-breakdown voltage are easier to trigger and thus have less variations in their run times. However, the jitter is also affected by the self-breakdown distribution and not just the fraction of median self-break voltage. This is because the actual fraction of self-break voltage varies statistically as does the self-break voltage. For example, a switch operating at 100 kV with a self-breakdown voltage distribution ranging from 110 to 150 kV will be operating between 67% and 91% of self-break voltage on any given charge cycle. A switch with a narrow self-breakdown distribution is highly desirable. In fact, in many cases, the relative width of the self-break voltage distribution is more important than the mean of the distribution [11].

(ii) The spread in switch operating point, manifested as a distribution in the self-break voltage, is caused by variations in the electrode conditions. By the nature of their operation, spark gaps impart roughness to the electrodes. Strongly electronegative gases such as SF_6 are affected by surface conditions, particularly at high pressures. At high pressures in nonuniform field geometries, reduced ion mobility limits the shielding effect, and in some cases the holdoff strength of electronegative gases actually decreases with higher pressure [12–14].

(iii) For reliable triggering, it is desirable to enhance the electric field near the location of the trigger plasma. However, for self-break voltage stability, a deenhanced (concave) gap is desirable to reduce the peak electric field of arc-damaged areas. As a compromise, uniform gap geometries have appeal to limit the overall (undesired) enhancement due to electrode damage, and to maintain a reasonable (desired) enhancement for the trigger mechanism. Notably, the total inductance for a given peak electric field is minimized in a uniform electric field geometry.

(iv) Cylindrical switches are generally more easily fabricated than other geometries, and for that reason are the most common. The outer diameter of the switch envelope has an effect on the inductance of the switch. Because the gas envelope insulator requires a larger gap than the triggered region (surface flashover strength is generally less than bulk insulator strength), there is an inductance penalty associated with that increased gap, and with the transition to the larger gap. That inductance penalty is reduced when the insulator transition is moved to a larger radius. The shunt capacitance of the switch electrodes helps to compensate for the arc inductance to some extent, and also provides electrostatic energy within a fraction of a nanosecond to heat the spark channel after triggering.

(v) There is a reduction in mean breakdown strength with increasing area, as the likelihood of a significant surface field enhancement increases [7]. There is an asymptotic breakdown strength value for large area electrodes at a given pressure. For moderate pressures in SF_6 (100–500 kPa), the breakdown strength is within a few percent of the asymptotic value for areas greater than a few thousand cm^2 for typical surface roughness. There is an appreciable increase in breakdown field for areas of 100 cm^2 or less, but the inductance of a switch with a relatively small diameter would be larger. Most commercial spark gaps use areas under 100 cm^2, and so operate at higher electric fields than a large switch, but generally with higher total inductance.

A desirable pulse generator system should have a low prefire rate, low jitter, and fast rise time simultaneously. In many systems, low jitter might practically mean a 1 standard deviation timing jitter 1 order of magnitude smaller than the rise time, for essentially negligible jitter. This dictates a system that has a strong trigger mechanism that strongly initiates the output switch closure at a relatively low fraction of its self-breakdown voltage. The distribution of self-break voltage at a given pressure can be used to predict the reliability at lower voltages [8,9,15].

1. Electrically triggered high-pressure gas switches

Trigatron switches [16–19] create a discharge on or near the surface of one electrode (usually the anode) with an auxiliary trigger pin located in that electrode. Those switches have relatively modest requirements for the magnitude of the trigger pulse (usually 10–30 kV, and nearly independent of the switched voltage [16]). The enhancement initiates a discharge streamer in the gas, which subsequently closes the main gap. Such switches are used in many systems, but it was decided based on published work that, without developmental effort, trigatrons would have

difficulty meeting the reliability and jitter requirements for this application simultaneously [20–22].

Field distortion switches [9,18,23–25] are used in systems requiring both low prefire rate and low jitter. To achieve both low prefire rate and low jitter from such a switch requires a trigger pulse comparable in amplitude to the switch voltage [26,27]. A triggered field distortion switch thus has power gain predominately through impedance reduction and not voltage increase. The problem then remains of raising the 5 V input pulse to a level suitable for triggering a 100 kV switch; for low jitter and high reliability the amplitude must be 50 kV or more.

The trigger pulse required for an electrically triggered switch could be generated in several ways. Marx generator circuits [28] and spiral generators [29] can be used to increase voltage above the switch charge level. Spiral generators, in particular, have been commonly used to generate trigger voltages for high-pressure spark gaps. While convenient, the relatively short and unpredictable usable lifetime of commercially available spiral generators, combined with the high output impedance, makes those systems undesirable in some cases.

A common technique used in some systems to generate high output voltages would be to use multiple stages of voltage amplification. These stages would include solid state, thyratron, and spark gap switches for the final output switch. Commercially available 100 kV DC-charged spark gaps have ~40 nH inductance, requiring multiple parallel switches to achieve the desired rise time. The number of stages (series and parallel) affects the total jitter, reliability, and misfire probability of the system.

2. Laser-triggered high-pressure switches

Laser triggering provides a convenient way to form a plasma channel in the electrically stressed region of a spark gap, in a period of time determined by the laser duration [30], which can be almost arbitrarily fast with short pulse lasers. Laser-triggered switches have used both plasma formation on an electrode, and plasma formation in the bulk insulator for initiating. Early laser triggering experiments used a long wavelength laser focused on one electrode for plasma formation and switch initiation. For the lowest jitter, it is desirable to create plasma in the bulk switch dielectric (in most cases high-pressure gas). This typically requires a shorter wavelength laser than plasma formation on an opaque switch electrode, but provides much larger field enhancement and therefore lower switch jitter. Moderately high-power, commercial pulsed ultraviolet lasers allow millimeter-length plasma channel creation in high-pressure gas, in a few nanoseconds. The plasma channel created from a cylindrical laser beam focused in the switch region provides a needle-shaped plasma with large field enhancement. The large field enhancement provides fast and accurate switch closure [26].

A large body of work exists on laser-triggered spark gap systems that switch with nanosecond accuracy [5,31–43]. Much of the work has been on systems of ~10 kV to drive optical Pockels cells, or in systems greater than 200 kilovolts for high peak power particle beam or x-ray generators. Despite the cost and complexity issues with high-power, fast-pulsed lasers, the advantages of laser triggering in some applications are considerable.

Sulfur hexafluoride gas has a relatively high electrical breakdown strength, and also has a relatively low threshold for plasma formation from ultraviolet light [38]. This conveniently maximizes spark gap holdoff voltage (for reduced inductance) and minimizes the laser energy required for triggering. The availability of relatively low-cost, frequency-quadrupled (266 nm) solid-state Nd:YAG lasers with low inherent jitter makes a laser-triggered system more practical than in the past. Modern commercial Q-switched lasers are available with subnanosecond jitter from the arrival of the input 5 V pulse to the coherent light output, delivering ~25 mJ in a three- to five-nanosecond pulse. Such lasers have been used for several years to control the multimegavolt gas switches in the *Z* pulser, and so have a history of performing well in a pulsed-power laboratory. The 25 mJ lasers used in this work can generate visible sparks of 15 mm length and ~0.1 mm diameter with an $f24$ system (300 mm focal length lens and a 12.5 mm diameter beam) with no applied electric field.

III. A LOW-INDUCTANCE TWO-CHANNEL LASER-TRIGGERED SPARK GAP

In most pulsed-power systems, the important performance parameters of a pulse generator are the temporal jitter of the output, the probability of a misfire, the output pulse amplitude and rise time, and the system maintenance interval.

To meet the system goals in the harsh mechanical and electromagnetic environment adjacent to the *Z* high current driver, we developed a low-inductance pulse generator with a high-pressure gas insulated, low-inductance laser-triggered switch. The system uses laser triggering in a nominally uniform electric field gap geometry. The switch uses two parallel arc channels to minimize inductance, reduce channel effective resistance, and reduce electrode arc damage. A single arc channel at SF_6 pressures less than 500 kPa would be too inductive to meet the rise time requirement. Multiple parallel switches would result in a larger and more complicated system.

A. Design

Figure 1 shows conceptual diagrams of the trigger pulser. Figure 1(a) shows the basic switch concept as implemented. Figure 1(b) shows a fully symmetric version of the switch with a set of output connectors for each switch half. The lower figure also shows an isolating inductor to force current sharing between channels. Figure 2 shows a sectional view of the actual system developed. In the system tested, the output feeds are dis-

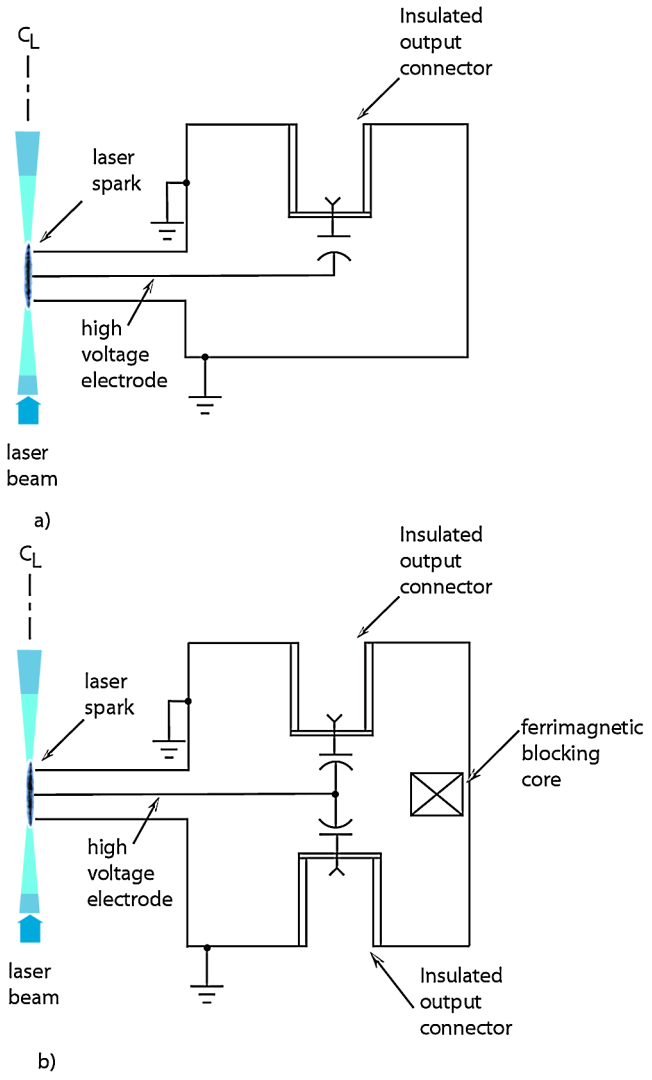

FIG. 1. (Color) Conceptual diagram of the two-channel laser-triggered pulse generator. The switch center plate is charged to high voltage. Current flows in two parallel laser-created spark channels to the grounded electrodes. The pulser system is axisymmetric (with the laser beam on axis) for lowest inductance. Upper figure: single-sided output. Lower figure: fully symmetric two sided output with blocking ferrite (see text).

crete axial conductors; power can flow from one switch half to the other. The ferrimagnetic core would prevent current flow from the upper output connector through the lower switch channel if one side of the switch closed before the other. If the jitter between the switch halves is small compared to the wave transit time between switch halves (as in the case of the system described here), the additional isolation is not needed.

During the initial design of the system, it was not known how well the channels would share current for the duration of the output pulse. The isolating inductor has not been necessary or tested here, although it may potentially reduce sensitivity to the location of the laser produced plasma by allowing more time before voltage falls on the later switch

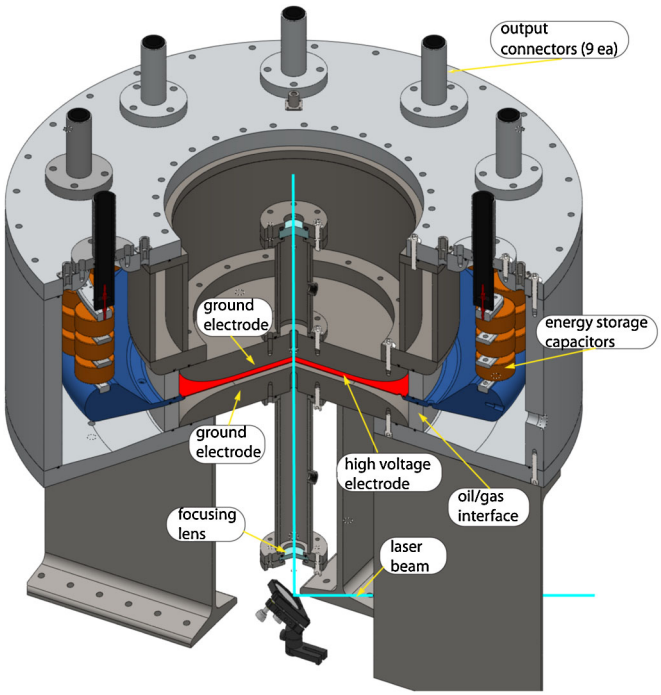

FIG. 2. (Color) The laser-triggered low-inductance switch and pulse generator system. The electrode gap in the center is 7 mm.

half. The required volt-second product would be determined by the timing jitter between the switch halves; relatively small cores of a few square cm cross sectional area would be adequate for the worst jitter we have observed.

The switch body is 873 mm in diameter. A cross-linked polystyrene [44] insulator with 400 mm inner diameter separates the high-pressure gas from the mineral oil insulated capacitor section. The capacitors are 2.6 nF, 40 kV strontium titanate ceramic units in a stack of three parallel sets of three series units, for a total of 2.6 nF at 120 kV rated voltage for each of the nine output cables (130 ns time constant). At 83% rated voltage, the capacitors maintain 95% of their rated capacitance. There are 81 capacitors total in the system. Grading resistors (1 GΩ) shunt the capacitors to ensure even voltage distribution. The electric field in the oil insulated DC-charged section is maintained at or below 4 kV/mm at 100 kV charge voltage. The energy storage capacitors form the center conductor of a triaxial oil insulated feed, which allows lower inductance than a coaxial feed. Because of its azimuthally distributed nature and the relatively large distance from the axis, the total inductance of the capacitor set is 2 nH. The current through the bottom switch flows on the outer feed gap. The lower impedance of the larger diameter outer feed tends to offset the longer path length to the lower switch. The output connectors are dry; the insulating oil does not contact the output cables. No breakdowns have been observed at the output cable connectors in the ten thousand full voltage shots performed.

Because the system has two grounded terminals with a high voltage midplane electrode, the system does not require insulating rods in tension. The cross-linked polystyrene gas-oil insulators are preloaded by deflection of the top metal plate of the housing to withstand the 244 kN pressure force at 860 kPa rated pressure. The balanced power flow design also eliminates stray electromagnetic fields from the charging and closure of the switch. Except for the output cables and the charge cable, the unit can be completely electrically isolated, and is completely enclosed.

The electrode materials are all 304L stainless steel. Replaceable arc region inserts were used on the prototype system but were judged unnecessary for the numbers of shots to be encountered in the Z facility ($\leq 10^5$). A thin (1 mm) midplane plate with a hole is charged to high voltage. The optical path penetrates one grounded electrode, through the hole in the midplane, then through a hole in the opposite grounded electrode. The optical focus is close to the middle of the midplane electrode. The focused laser beam creates a plasma channel in the gas extending from the high voltage midplane electrode towards both grounded electrodes. The focal point axial position is fine adjusted with a $3\times$ optical beam expander with divergence adjustment. The transported beam is expanded for reduced fluence on the optics, and for the divergence adjustment. In practice, the beam is adjusted until the top and bottom switches close at the same time, and the currents are the same. Current is measured with derivative-responding flux loops [45] mounted inside the top lid. Some leakage through the space between the nine output cables requires correction to remove the resultant crosstalk, which is of the order of 10%. Where the indicated currents are equal within 15%, the correction for crosstalk is negligible.

Switch inductance and channel resistance both promote current sharing between the two channels. For times comparable to an inductive time constant, which is $\sim$20 nanoseconds with 20 nH on each side of the switch, and 1 Ω channel resistance, inductance largely determines current sharing. The inductances on each side of the switch are close to equal; the lower switch feed has a longer transit length, but lower impedance. At later times, channel resistance is the dominant factor in current sharing. Because the spark channel properties are dominated by the electrostatic energy spent heating the channels in the first fractions of a nanosecond, the channels are likely to be similar in conductivity. If the channel resistances are similar, that resistance balance determines current sharing at later times.

The switch uses a single laser beam to create a laser spark closing two parallel spark gap switches. Because there is no appreciable mutual inductance between the switches, this immediately halves the inductance of the entire switch system. The 25 mJ laser pulse provides enough energy to create a plasma channel with adequate extent to close both switches with a 300 mm focal length lens and a 12.5 mm diameter laser beam. Shorter focal length systems have higher specific optical energy density in a shorter and more intense spark; longer focal lengths tend to make longer but more tenuous sparks. There are also more shot to shot spark length variations with longer focal lengths. We have not optimized the focal length for minimizing trigger optical energy with this switch, but believe the optimum is in the range 300 to 700 mm for the laser employed here. The laser spark must extend most of the way through two 7 mm gaps and the 1 mm thick center plate for closing both gaps with subnanosecond simultaneity. Concepts to refocus light exiting the switch, or extending the laser spark with aspheric optics, could reduce the required laser energy and have been considered but not implemented here. Because the laser beam path exits the switch, it is possible to monitor the optical energy not dissipated or dispersed in the switch focus.

About half of the incident ultraviolet laser energy exits the switch coherently through the opposite grounded electrode. Most of the lost light is presumably scattered, so the energy available for ionization of the switch gas is 0.5 millijoules per mm or less. Assuming a spark column 0.1 mm in diameter and 15 mm long, the average laser energy dissipated is about 2.5 eV/molecule average at 400 kPa pressure. The laser produced plasma is thus weakly ionized and relatively cold [46]. The absorbed optical energy ($\sim$ 3.5 mJ) is small compared to the electrostatic energy stored in the switch electrode region ($\sim$ 800 mJ), so substantial resistive heating occurs to create significant conductivity. The laser spark simply initiates the plasma channel; it is electrostatic energy that actually forms the low resistance channel that carries significant current.

As an alternative to the design shown here, a single laser beam could be split optically and routed to multiple independent switches. However, a beam splitting system would have considerably more optical components and would be more difficult to align. Each antireflection coated optical surface reduces the beam energy several percent. The use of a single laser spark to close both switches reduces the complexity of the optical path, and reduces the number of optics surfaces that reduce energy, can get dirty, and must be aligned. With both arc channels centered on the same axis, there is negligible mutual inductance between the channels. Other work on multiple spark channels in a single switch [47,48] had appreciable mutual inductance between the channels, which limited the reduction in total effective inductance.

In the switch described here, the multiple channels are transit time isolated (by five or more times greater than the switch jitter) to allow reliable closure of both channels even without the isolating inductor. Besides lower inductance, an additional benefit of multiple channels is reduced erosion. Because of the isolation between channels, the current sharing is close to uniform, so each channel carries

half the total current, substantially reducing the electrode erosion [49]. Reduced erosion is important for cleanliness inside the switch; debris can affect the insulator surfaces and the optical windows.

As noted before, there are two issues with high-pressure spark gap switch performance. At the highest pressures, the self-breakdown electric field has more variations because electrode damage and defects are larger compared to the electronegative gas shielding distance—essentially, the electrodes are more enhanced at higher pressures. The mean electric holdoff strength (V/mm/Pa) also falls at higher pressures in geometries with field enhancements, and so high pressures can be problematic for systems with nonuniform fields (as can be caused by the laser entrance holes, and arc damage). Addressing both of these issues was accomplished by using a 7 mm electrode gap to maximize the linear range of the self-break versus pressure curve, while maintaining reasonable inductance.

B. Results

1. Operating pressure

The initial version of the pulser had the option of 4, 6, and 8 mm gaps. As expected, the smallest gaps required the highest pressures for a given voltage holdoff. In terms of electric field, the different gaps behave similarly at low pressures. At higher pressures, the 4 mm gap self-breakdown voltage becomes sublinear with pressure, and the fractional variation in self-breakdown voltage (spread) becomes large. Figure 3 shows the self-breakdown voltage versus pressure for 4, 6, and 8 mm in pure SF_6. The system was limited in total voltage, and so at the larger gaps only lower pressures could be investigated. While the smaller gap would allow lower inductance, the variations in self-breakdown voltage were deemed unacceptably high for a stable, low jitter system. For that reason, the system in routine use employs 7 mm gaps, and operates at 14.3 kV/mm average field and 432 kPa pure SF_6. No prefires or misfires have been observed under these conditions in the course of approximately 10 000 shots.

Quantifying the prefire probability of a gas switched system such as this is useful, and can be done in at least three ways: The first and most straightforward method is to operate the system normally, and observe prefires over a number of shots. This can be time consuming because of the number of shots required for systems with 10^{-4} or lower prefire probability. The large number of shots may also cause significant conditioning or erosion, and so could affect the results. The second method is to operate the system at higher than normal voltage, and characterize the self-break distribution function at the operational pressure. The rest of the system must be able to tolerate the higher voltages; this can be a problem for low inductance designs where electric fields are relatively high during normal voltage operation. The results at higher than normal voltage may be pessimistic if the higher voltage introduces new switch closure modes. The third way to characterize the prefire probability is to characterize the self-breakdown distribution with smaller gaps, at normal voltage and pressure. This can be accurate if the electric fields are not affected by the gap change, which is true for nominally planar electrodes. This test method limits voltage stress to normal levels.

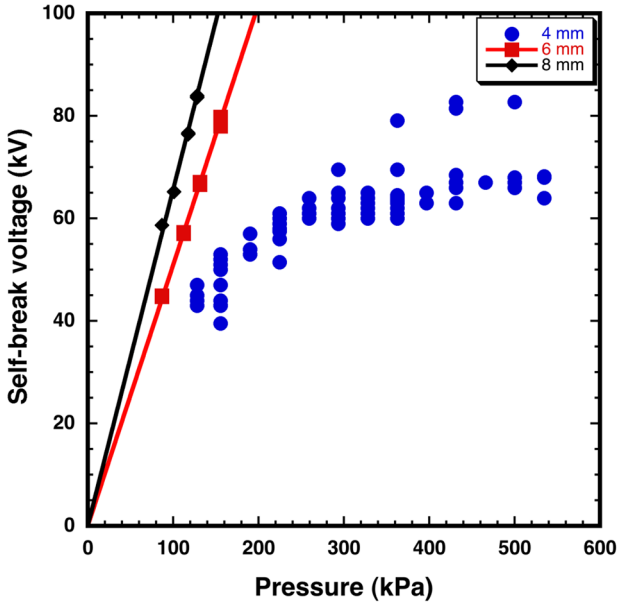

FIG. 3. (Color) Self-breakdown voltage versus pressure in pure SF_6 for 4, 6, and 8 mm gaps. The variations in self-breakdown voltage are more pronounced at higher pressure. The slope ratio of the two fitted lines (6 and 8 mm) is 1.29; the ratio of the gaps is 1.33, indicating reasonably linear SF_6 insulating behavior at those pressures and gaps.

Scaled reliability calculations were done for the switch shown here at reduced gap values. The self-breakdown data with a 4 mm gap were scaled to the operational 7 mm gap linearly. The calculations were done for three different pressures. A largest extreme value fit was chosen based on comparison of the fit quality. Figure 4 shows the cumulative self-breakdown distribution function generated from a largest extreme value fit to the self-breakdown voltage at three pressures (362, 432, and 500 kPa). The calculated nominal voltage for 10^{-5} failure rate at 432 kPa is 101 kV; the 95% confidence interval spans the range 92 to 110 kV for 10^{-5} failure rate at that pressure. The 10^{-3} failure rate voltage range is 97 to 111 kV (95% confidence) with a nominal value of 104 kV, based on the self-break data. The median self-break voltage is 119.7 kV at 432 kPa; the switch operates reliably at 84% of the *median* self-break voltage. The calculations are based on a relatively small number (~ ten) self-breakdown tests. The uncertainty could be reduced appreciably with a larger number of self-breakdown measurements. The largest extreme value (or Gumbel) distribution [50] is the largest values from a set of probabilities. The largest extreme value

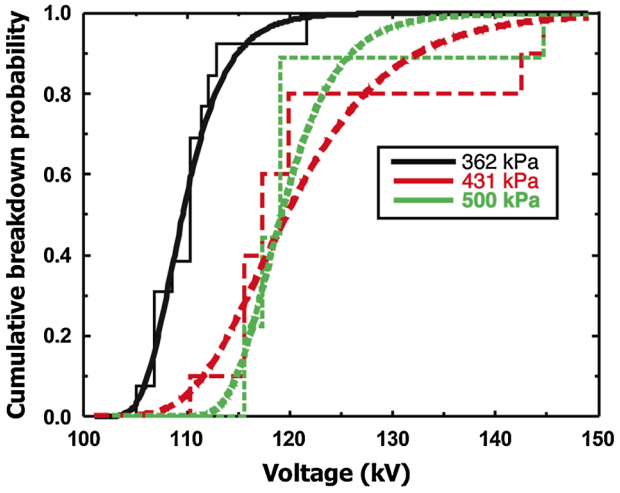

FIG. 4. (Color) Cumulative breakdown probability plot for 362, 431, and 500 kPa SF6 pressure, generated from a largest extreme value model fit to the self-breakdown voltage data at three pressures, shown with self-break data (stairstepped). Data are taken with 4 mm electrode gap, and shown scaled linearly to the operational gap of 7 mm. The calculated prefire probability at 431 kPa and 100 kV is less than 10^{-5}.

distribution has a probability function of

$$PDF(x, \alpha, \beta) = \frac{\exp[\exp(\frac{-x+\alpha}{\beta}) + \frac{-x+\alpha}{\beta}]}{\beta}, \qquad (1)$$

here α and β are fitted parameters and x is the independent variable [51]. The exponential of an exponential accounts for a distribution of failures resulting from a distribution of failure mechanisms. The largest extreme value model produces better fits when there are occasional high valued results, such as the small number of very high self-break voltages present in the data. High values can be observed in the initial tests due to pristine electrodes (the data have not been correlated with electrode life; the results are equally weighted). The presence of occasional very high voltage self-breakdowns scarcely adds to the reliability of the switch, but adds to the undesirable width of the self-break distribution. Large holdoff conditions also typically increase triggering difficulty, essentially increasing jitter.

Figure 5 shows the calculated prefire probability from a best fit of a largest extreme value function to the self-break data at 432 kPa pressure. The data were acquired with a 4 mm gap, and scaled to the operational 7 mm gap.

2. Output performance and spark gap resistance

Figure 6 shows output voltage measured by multiplying the output current by the load impedance, for both pure SF_6 in the switch and 90% nitrogen with 10% SF_6. Figure 7 shows the channel resistance calculated from the output voltage, the known circuit values, and the initial charge voltage. The channel resistance can be calculated from the circuit, ignoring wave transit times in the pulser:

$$R_{\text{channel}} = Z_{\text{load}} - \frac{V_0}{I} + \frac{1}{IC}\int_{-\infty}^{t} I d\tau + \frac{L}{I}\frac{dI}{dt}, \qquad (2)$$

where Z_{load} is the external load impedance, V_0 is the initial DC charge voltage on the capacitor, I is the total circuit

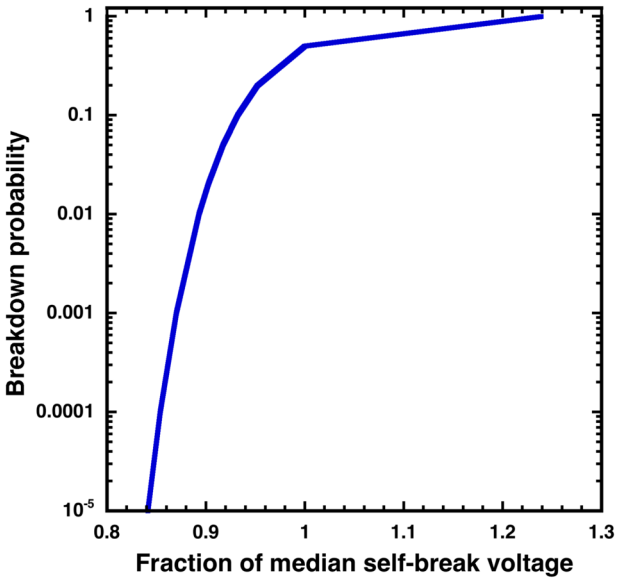

FIG. 5. (Color) Logarithmic plot of calculated prefire probability versus fraction of *median* self-break voltage at 432 kPa, with 7 mm gaps, calculated from a largest extreme value fit to the measured self-break data. By definition, the breakdown probability at the median self-break voltage is 0.5.

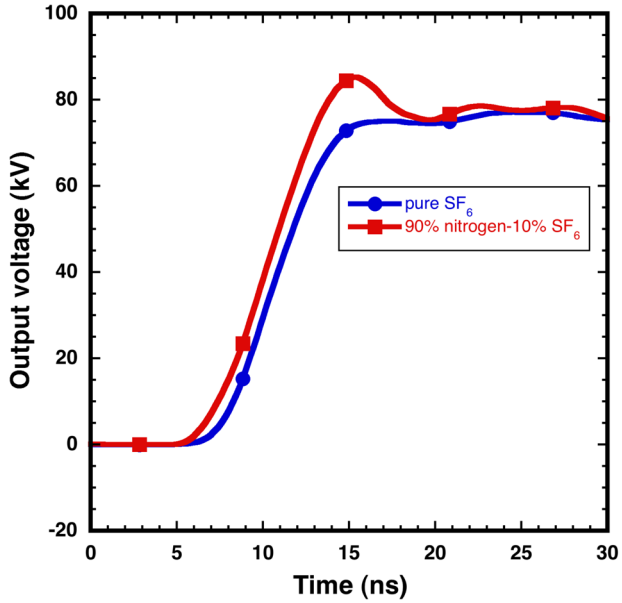

FIG. 6. (Color) Voltage output from pulser with pure SF_6 (circles) and a mixture of 90% N_2 and 10% SF_6 (squares). The tests were done at the same fraction of self-break voltage, and at 100 kV DC charge.

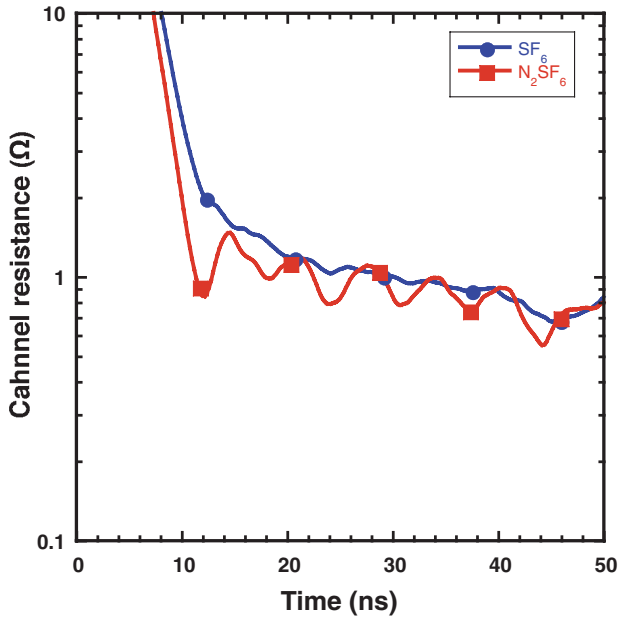

FIG. 7. (Color) Arc channel resistance for pure sulfur hexafluoride and 90% nitrogen-10% sulfur hexafluoride mixture.

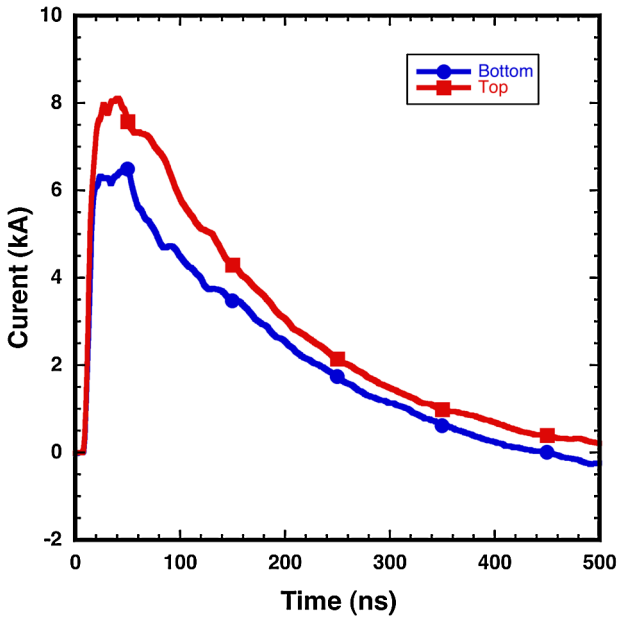

FIG. 8. (Color) Currents measured on each half of the switch system.

current, and L is the circuit inductance. Figure 7 shows calculated channel resistance for the two channels with pure SF6 and a 90% nitrogen, 10% SF6 mixture at the same fraction of median self-break voltage. The resistance for the nitrogen mixture is significantly lower at early times, allowing somewhat higher peak voltage and faster rise time with the nitrogen mixture. The plateau resistance is similar for the two gases. This could imply that the channel expansion in the lighter mixture results in cooling and higher plasma resistivity [52]. In this system, the spark resistance has an appreciable effect on the output amplitude.

The channel resistance is the combined effective resistance of the two channels carrying part of the total current. Figure 8 shows the currents measured on the top and bottom halves of the switch. Martin [53] assumes the combined effective resistance of channels carrying equal currents to be proportional to $n^{-1/3}$. In that case, the resistance of a two-channel switch would be 79% that of a single channel. Kushner [48] predicts a lowering of total resistance as $n^{-2/5}$, which would make the effective resistance of two channels 76% that of a single channel. Switch conductance is sublinear with the number of channels because less energy is available to heat the channel when the current is divided, so the channel is a combination of lower temperature and smaller diameter. The drop in resistance is beneficial, even though it does not scale directly with the number of channels.

Figure 9 shows a circuit model of the two switch halves. We assume for simplicity that the resistance of one side is the product of a scale factor and the resistance of the other switch half; that scale factor is allowed to vary as a function of time. If the current were shared perfectly, the scale factor would be unity. With current measured on both halves of the switch, and neglecting transit time between the switch halves (3.2 ns), the ratio of the two resistors can be found to be

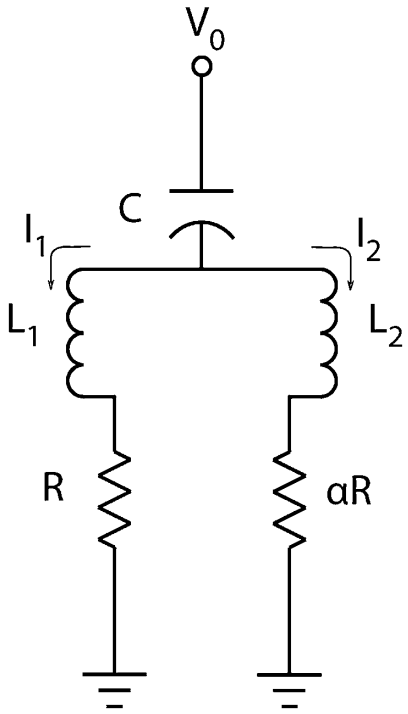

FIG. 9. Schematic of the two switch halves and the circuit model components.

$$\alpha = \frac{I_1}{I_2} - \frac{1}{RI_2}\left[L_1\frac{dI_1}{dt} - L_2\frac{dI_2}{dt}\right], \quad (3)$$

where R is the nominal spark resistance on each side, L_1, L_2 are the switch half inductances, α is the resistance scale factor, and I_1, I_2 are the measured switch half currents. Current is observed to flow on both halves of the switch for the entire 500 ns full width of the output pulse. If the laser alignment is such that one side of the switch closes before the other, the first channel carries more current. The earliest channel to close carries proportionately more current later in time. The channels are expanding in diameter with time [6,52,54] and Ohmically heated by the conducted current. Figure 10 shows relative channel resistances for the two switch halves for the entire pulse duration.

Figure 11 shows output voltage for normal dual channel operation, and for single channel operation induced by translating the laser focus so that one side carries more than 90% of the total current. The output rise time is 7.0 ns for single channel operation, and 4.4 ns for dual channel switching. The rise time is not exactly doubled for single channel operation because of channel resistance, and the compensating effect of the capacitance of the inactive side in single channel mode.

Figure 12 shows the calculated resistances for dual channel operation and single channel operation. The total resistance falls more quickly for two-channel operation, but again the plateau resistance is similar for the two cases.

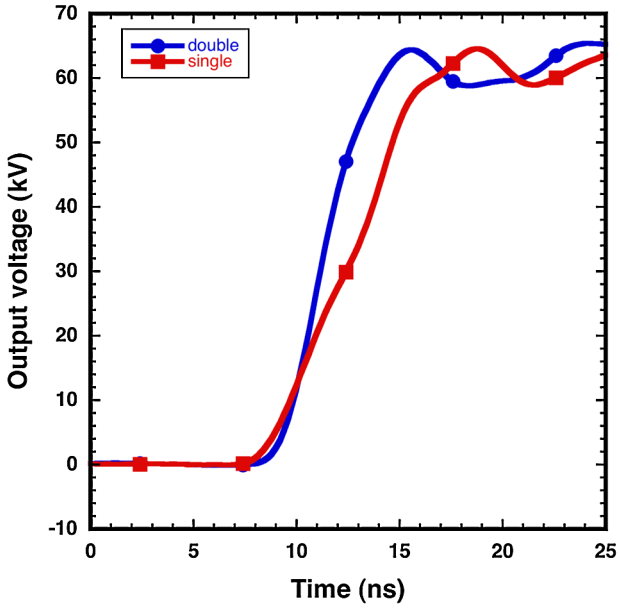

FIG. 11. (Color) Output voltage with normal two-channel operation, and with the laser focal point adjusted so that one side of the switch closes later than the other, so that 95% of the current flows on one side, effectively acting as a single channel switch. As expected, the rise time is shorter by nearly a factor of 2 with both channels. The shunt capacity of the nominally unused switch half in the single channel case may act to compensate the channel inductance and raise the output voltage above the level of a conventional single-sided switch. The tests were done at 77 kV DC charge.

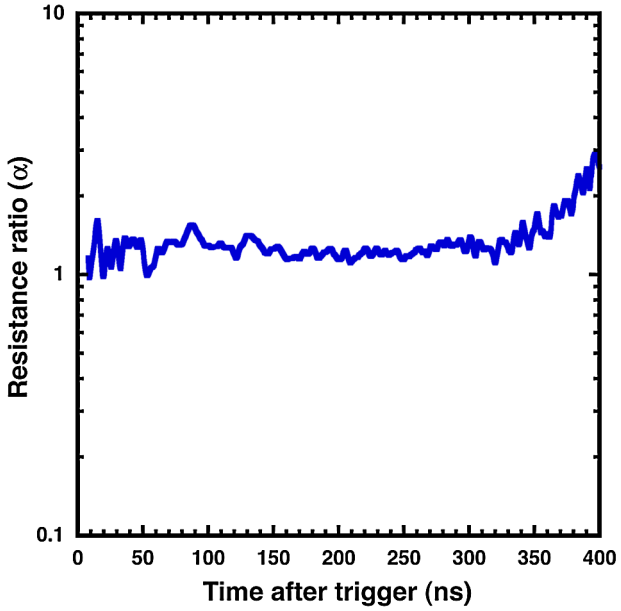

FIG. 10. (Color) Ratio of the top channel resistance to the bottom channel resistance. The channels share current consistently. Calibration and spurious noise issues may affect the calculation to some extent; the inflection at 325 ns is largely due to numerical issues with currents close to zero.

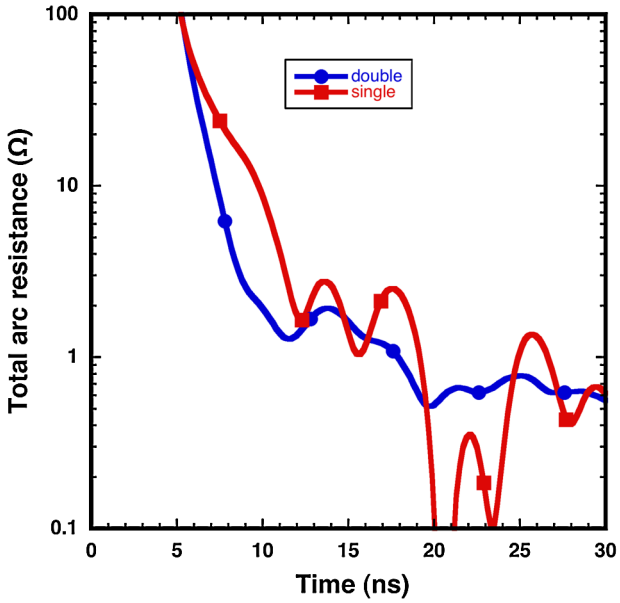

FIG. 12. (Color) Calculated resistance in normal mode with both sides conducting current, and with most of the current flowing on one side of the switch. Displacement current to the inactive side of the switch affects the calculated single channel resistance at 20 ns.

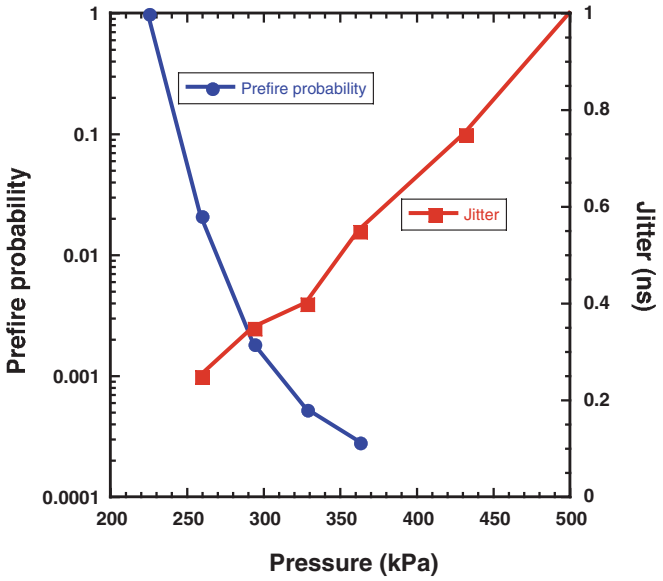

FIG. 13. (Color) Prefire probability and system jitter, versus switch pressure at 100 kV charge voltage. Data are shown for pure SF6. Roughly 10 000 shots were acquired to generate this plot.

3. Timing performance

The pulser system was tested extensively in a sophisticated, unattended automated tester that performed a gas purge, set pressures and voltage levels, and charged and triggered the system. A voltage drop anytime before triggering was recorded as a prefire. The system recorded voltage and current derivative waveforms as well as laser energy from a calorimeter, and pressure and voltage of the system just before triggering. Figure 13 shows the measured charge cycles between prefires as a function of switch pressure, and the 1 standard deviation timing jitter as a function of switch pressure. Figure 14 shows a histogram of switch closure timing relative to the laser optical pulse on a continuous series of *Z* system shots. The timing standard deviation is 430 ps. The data sample time, τ_{sample}, is 200 ps per point, which adds 140 ps one-sigma ($\frac{\tau_{\text{sample}}}{\sqrt{2}}$) uncertainty to the timing in quadrature. The result is an estimated 407 ps switch jitter. Figure 15 shows a timing variation histogram for the laser [55] alone. The timing one-sigma deviation of the laser itself is 375 ps. The net system timing uncertainty is therefore 553 ps at the normal operating pressure of 432 kPa and 100 kV charge, including the laser and the switch.

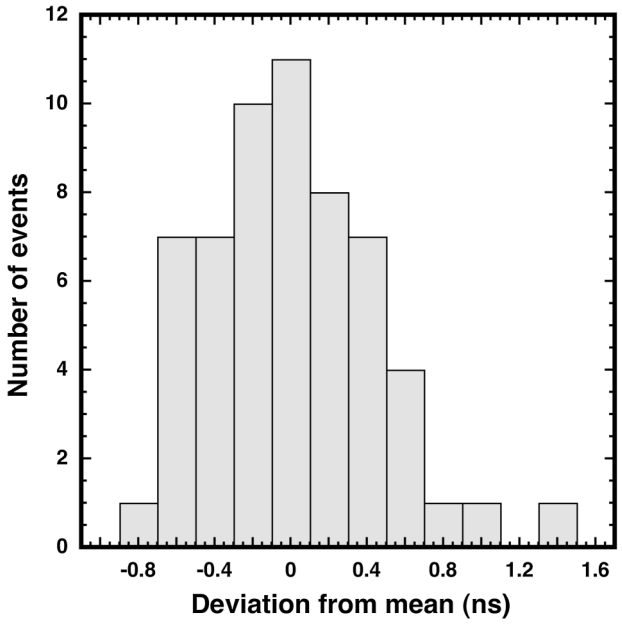

FIG. 14. Histogram of pulse generator run time relative to the laser photodiode signal on full system shots of the *Z* facility. The 1 standard deviation in the timing is 430 ps. This includes digitizer uncertainty, which is of the order of 140 ps, at 200 ps per point sampling rate.

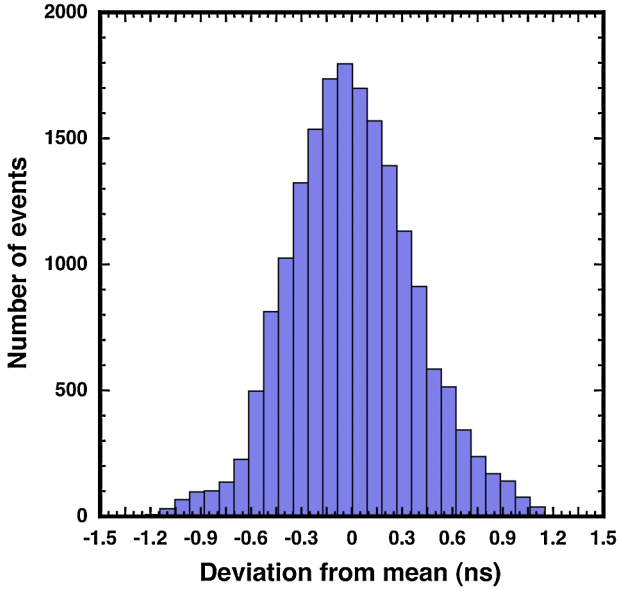

FIG. 15. (Color) Jitter of the laser itself: deviation from the mean of measured 532 nm leakage light from the trigger laser relative to a fast-rising (100 ps) trigger signal. Data are acquired on 18 000 consecutive laser-only shots, sampled at 20 ps per point. The 1-σ standard deviation of the laser output with respect to its trigger is 375 ps.

IV. CONCLUSIONS

We have shown the design and results from a laser-triggered high voltage pulse generator that drives a 5.56 Ω resistive load with 80 kV, a 6 ns 10%–90% rise time, 550 ps jitter, and less than 10^{-4} misfire probability at the same time. The system uses a single optical path to initiate two spark channels. The system stores 117 J at 100 kV. The switch closure is initiated by 25 mJ of 266 nm laser light in a 3–5 ns FWHM pulse. The total system inductance (including switch, capacitors, output connec-

tions) is 14 nH, using a 300 mm diameter nearly uniform-field switch. The prefire probability of the switch has been studied extensively because of the critical need for a highly reliable system. The relatively low jitter and fast rise time are combined with a low prefire probability, to make a system that has been used effectively in a large pulsed-power driver as the primary trigger generator.

ACKNOWLEDGMENTS

The authors would like to thank Dr. D. E. Bliss and Dr. J. R. Woodworth for generous and invaluable advice on the optical system. D. Spencer and P. Wakeland did an outstanding job designing the mechanical components for the deployed system and the prototype. The authors are also indebted to Dr. J. E. Maenchen for having the foresight to allow the development work to be conducted, and to Dr. W. A. Stygar for continual encouragement of the effort. Sandia is a multiprogram laboratory operated by Sandia Corporation, a Lockheed Martin Company, for the United States Department of Energy's National Nuclear Security Administration under Contract No. DE-AC04-94AL85000.

[1] F. J. Zutavern, S. F. Glover, K. W. Reed, M. J. Cich, A. Mar, M. E. Swalby, T. A. Saiz, M. L. Horry, F. R. Gruner, and F. E. White, IEEE Trans. Plasma Sci. **36**, 2533 (2008).

[2] F. Barbosa, P. A. Arnold, G. B. McHale, G. James, G. Brown, E. G. Cook, and B. C. Hickman, *2008 IEEE International Power Modulator Conference, Las Vegas* (IEEE, Piscataway, NJ, 2008), p. 109.

[3] C. A. Pirrie and H. Menown, *Power Modulator Symposium, Norfolk, VA* (IEEE, Piscataway, NJ, 2000), p. 9.

[4] N. C. Jaitly, M. D. Coleman, A. Ramrus, S. Eckhouse, L. M. Earley, J. N. Downing, H. H. Reisch, L. D. Caudill, S. A. Eversol, and G. Barnes, *Power Modulator Symposium, Myrtle Beach, SC* (IEEE, Piscataway, NJ, 1992), p. 227.

[5] K. R. LeChien, M. E. Savage, V. Anaya, D. E. Bliss, W. T. Clark, J. P. Corley, G. Feltz, J. E. Garrity, D. W. Guthrie, K. C. Hodge, J. E. Maenchen, R. Maier, K. R. Prestwich, K. W. Struve, W. A.Stygar, T. Thompson, J. V. D. Avyle, P. E. Wakeland, Z. R. Wallace, and J. R. Woodworth, Phys. Rev. ST Accel. Beams **11**, 060402 (2008).

[6] W. D. Kimura, M. J. Kushner, E. A. Crawford, and S. R. Byron, IEEE Trans. Plasma Sci. **14**, 246 (1986).

[7] T.Nitta, N. Yamuda, and Y. Fujiwara, IEEE Trans. PAS **pas-93**, 623 (1974).

[8] A. L. Donaldson, M. O. Hagler, M. Kristiansen, L. L. Hatfield, and R. M. Ness, J. Appl. Phys. **57**, 4981 (1985).

[9] I. D. Smith, Physics International Internal Report No. PISR-127-4, 1969.

[10] B. N. Turman and D. R. Humphreys, *6th IEEE International Pulsed Power Conference, Arlington, VA* (IEEE, Piscataway, NJ, 1987), p. 347.

[11] J. J. Ramirez, J. Appl. Phys. **47**, 1925 (1976).

[12] M. Zwicky, IEEE Trans. Electr. Insul. **ei-22**, 317 (1987).

[13] Y. Qui and I. D. Chalmers, J. Phys. D **26**, 1928 (1993).

[14] A. H. Cookson, *Third International Conference on Properties and Applications of Dielectric Materials, Tokyo, Japan* (IEEE Press, Piscataway, NJ, 1991).

[15] A. L. Donaldson, M. Kristiansen, A. Watson, K. Zinsmeyer, and E. Kristiansen, IEEE Trans. Magn. **22**, 1441 (1986).

[16] P. F. Williams and F. E. Peterkin, in *Gas Discharge Closing Switches*, edited by G. Schaefer, M. Kristiansen, and A. Guenther (Plenum, New York, 1990), Vol. 2, p. 63.

[17] J. D. Craggs, M. E. Haine, and J. M. Meek, J. Inst. Electr. Eng. **93**, 963 (1946).

[18] J. C. Martin, Proc. IEEE **80**, 934 (1992).

[19] S. J. MacGregor, F. A. Tuema, S. M. Turnbull, and O. Farish, IEEE Trans. Plasma Sci. **25**, 118 (1997).

[20] M. D. Williams, NASA Internal Report No. TN D-5077, 1969.

[21] E. Thornton and I. D. Somerville, *Pulsed Power Conference, Monterey, CA* (IEEE, Piscataway, NJ, 1989), p. 543.

[22] R. E. Beverly and R. N. Campbell, Rev. Sci. Instrum. **67**, 1593 (1996).

[23] G. Schaefer, in *Gas Discharge Closing Switches*, edited by G. Schaefer, M. Kristiansen, and A. Guenther (Plenum, New York, 1990), Vol. 2, p. 85.

[24] P. M. Barnes, J. E. Gruber, and T. E. James, J. Sci. Instrum. **44**, 599 (1967).

[25] R. S. Post and Y. G. Chen, Rev. Sci. Instrum. **43**, 622 (1972).

[26] T. H. Martin, *5th IEEE International Pulsed Power Conference, Arlington, VA* (IEEE, Piscataway, NJ, 1985), p. 74.

[27] T. H. Martin, *7th IEEE International Pulsed Power Conference, Monterey, CA* (IEEE, Piscataway, NJ, 1989), p. 73.

[28] R. A. Fitch, IEEE Trans. Nucl. Sci. **18**, 190 (1971).

[29] F. Rühl and G. Herziger, Rev. Sci. Instrum. **51**, 1541 (1980).

[30] J. M. Meek and J. D. Craggs, *Electrical Beakdown of Gases* (John Wiley and Sons, New York, 1978).

[31] A. J. Alcock, M. C. Richardson, and K. Leopold, Rev. Sci. Instrum. **41**, 1028 (1970).

[32] D. J. Bradley, J. F. Higgins, M. H. Key, and S. Majumdar, Opto-Electron. **1**, 62 (1969).

[33] A. H. Guenther and J. R. Bettis, J. Phys. D **11**, 1577 (1978).

[34] M. Hasselbeck, L. Huang, S. C. Hsu, and K. S. Kwok, Rev. Sci. Instrum. **54**, 1131 (1983).

[35] M. J. Kushner, R. D. Milroy, and W. D. Kimura, J. Appl. Phys. **58**, 2988 (1985).

[36] J.-L. Parpal, H. P. Mercure, and G. R. Mitchel, IEEE Trans. Electr. Insul. **24**, 1191 (1989).

[37] W. K. Pendleton and A. H. Guenther, Rev. Sci. Instrum. **36**, 1546 (1965).

[38] W. R. Rapoport, J. Goldhar, and J. R. Murray, IEEE Trans. Plasma Sci. **8**, 167 (1980).

[39] K. Schildbach and D. Basting, Rev. Sci. Instrum. **45**, 1015 (1974).

[40] J. R. Woodworth, R. G. Adams, and C. A. Frost, IEEE Trans. Plasma Sci. **10**, 257 (1982).

[41] J. R. Woodworth, C. A. Frost, and T. A. Green, J. Appl.

Phys. **53**, 4734 (1982).
[42] J. R. Woodworth, P. J. Hargis, L. C. Pitchford, and R. A. Hamil, J. Appl. Phys. **56**, 1382 (1984).
[43] W. Worts and S. D. Koveleski, *IEEE Pulsed Power Conference, Monterey, CA* (IEEE, Piscataway, NJ, 2005). p. 623.
[44] C-Lec Plastics Internal Report, ''Rexolite 1422.''
[45] D. G. Pellinen, Rev. Sci. Instrum. **42**, 667 (1971).
[46] A. G. Akmanov, L. A. Rivlin, and V. S. Shil'dyaev, JETP Lett. **8**, 258 (1968).
[47] O. Frolov, K. Koláček, J. Schmidt, J.Štraus, and V. Prukner, Czech. J. Phys. **56**, B218 (2006).
[48] M. J. Kushner, W. D. Kimura, D. H. Ford, and S. R. Byron, J. Appl. Phys. **58**, 4015 (1985).
[49] A. L. Donaldson, in *Gas Discharge Closing Switches*, edited by G. Schaefer, M. Kristiansen, and A. Guenther (Plenum, New York, 1990), Vol. 2, p. 325.
[50] E. J. Gumbel and J. Lieblein, The American Statistician **8**, 14 (1954).
[51] M.Aitkin and D. Clayton, Appl. Statist. **29**, 156 (1980).
[52] M. J. Kushner, W. D. Kimura, and S. R. Byron, J. Appl. Phys. **58**, 1744 (1985).
[53] J. C. Martin, *J. C. Martin on Pulsed Power* (Plenum, New York, 1996).
[54] W. D. Kimura, M. J. Kushner, and J. F. Seamans, J. Appl. Phys. **63**, 1882 (1988).
[55] Tempest-10 Laser System (New Wave Research, 48660 Kato Road, Fremont, CA 94538).